Chemical Vapor Depositions of Single-Walled Carbon Nanotubes Catalyzed by Uniform Fe_2O_3 Nanoclusters Synthesized Using Diblock Copolymer Micelles

Qiang Fu, Shaoming Huang, and Jie Liu*

Gross Chemistry Laboratory, Duke University, Box 90354, Durham, North Carolina 27708

Received: February 4, 2004; In Final Form: March 17, 2004

Inversed micelles formed by polystyrene-*block*-poly(2-vinyl-pyridine) in toluene loaded with $FeCl_3$ were used to synthesize and deliver discrete Fe_2O_3 nanoclusters with uniform diameters to flat substrates. Single-walled carbon nanotubes (SWNTs) were grown by chemical vapor deposition using these nanoclusters as the catalysts. Atomic force microscope characterizations revealed that high density SWNT mats were grown on the surface and the diameter of nanotubes was controlled by the diameter of nanoclusters. Electrical measurement revealed that the dense SWNT mats contained both semiconducting and metallic SWNTs and could be used to build thin film transistors.

Introduction

Since Iijima's discovery of the carbon nanotube in 1991,[1] carbon nanotubes have been intensively studied in chemistry, physics, and materials science. Single-walled carbon nanotubes (SWNTs) are formed by single layer of graphenes and can be either semicondcuting or metallic depending on the helicity and diameter.[2] Due to their unique one-dimensional structures, SWNTs have high potentials in many technological applications. In past decades, SWNTs have been used to build field effect transistors,[3] chemical sensors,[4] infrared emitters,[5] and logic circuits.[6,7] Quantum effects related with one-dimensional structures such as the kondo effect,[8] luttinger liquid behavior,[9] and Aharonov−Bohm oscillations[10] have also been reported experimentally. Meanwhile, high quality SWNTs films have also been used to build chemical sensors[10−12] and thin film transistors[13] that showed high application potentials. All those applications require high quality SWNTs deposited on flat surfaces to fabricate high performance devices.

Chemical vapor depositions (CVD) of SWNTs has been proved to be a classic method to produce SWNTs. Compared to the arc discharge and laser ablation methods, CVD could offer more control over the growth temperature, catalyst composition, feeding gas, and other parameters.[14] More importantly, CVD enables SWNTs to be directly grown on a surface in a controllable fashion.[15,16] Recently, progress has been made in controlling the diameter of the SWNT using catalyst nanoclusters preformed by wet chemistry.[17−19] For example, SWNTs have been directly grown on flat surfaces using discrete Fe_2O_3 nanoclusters synthesized using ferritin as templates.[18] Preformed Fe and Fe/Mo[17,20−22] nanoclusters with different diameters were also used as the catalyst to grow SWNTs to control their diameters.[19,20] However, although those significant progresses have been made in the synthesis of uniform nanoparticle catalysts for SWNT growth, it is still a great challenge in making nanoclusters with different diameters in the range 1−10 nm with good control of their diameters. Additionally, nanoclusters may aggregate on a surface when they are transferred to the substrate, which is one of the main reasons that introduce variations in catalyst size for nanotube synthesis.

Here we report that we apply the polystyrene-*block*-poly(2-vinylpyridine) (PS−PVP) dicoblock copolymer micelles[23] loaded with iron(III) chloride as a precursor to prepare Fe_2O_3 nanoclusters and then use them as catalysts for SWNT growth in CVD. Compared to the previously reported methods, this new method is more attractive for several reasons: (1) The stability of the micelles and the method used to transform micelles into catalyst nanoculsters enable us to obtain high coverage of nanoclusters on the surface without aggregation. (2) Wide controllable size can be obtained by adjusting the ratio of the iron(III) chlorides and PVP block in the copolymer. (3) A relatively narrow diameter distribution of the micelle ensures diameter distributions of the nanoclusters in a very narrow range. (4) Convenient methods are developed to transfer the micelle to various substrate in large area by simple dip-coating or spin coatin.[23−25] We show that using this new method, we can conveniently obtain monodispersed nanoclustes on surface. Those nanoclusters could be used as the catalysts to synthesize high density SWNT mats on surfaces by CVD. Electrical measurements of those SWNTs mats prove that they are mixtures of semiconducting and metallic nanotubes and could be used to fabricate thin film transistors.

Experiments

Preparation of Micelles Loaded with Iron(III) Chlorides. A 25 mg sample of polystyrene (53800)-*block*-poly(2-vinylpyridine) (8800) (PS−PVP) (Polymer Source, Inc.) diblock copolymer was added to 25 mL of toluene, and the mixture was then stirred for more than 4 h. A 3.3 mg sample of $FeCl_3 \cdot 3H_2O$ (Fe^{III}:PVP = 0.6) was then added to the solution, and the resulting mixture was stirred at room temperature for 24 h. The final solutions were then stored in vials for future use. The solutions could be further diluted to obtain the micelles with low loading ratios (Fe^{III}:PVP = 0.2, 0.06) with blank micelle solutions and stirred for more than 48 h.

Preparation of Nanoparticles on Surface. The substrates used are n-type highly doped Si wafers with 1000 nm thermal oxide layers (Silicon Quest International, CA). The micelle solutions were first diluted 10 times by toluene and then dip-coated or spin-coated on the substrate at 8000 rpm (KW-4, Chemat Technology). The micelle film was then treated with

* To whom should be corresponded. E-mail: jliu@chem.duke.edu.

10.1021/jp049483+ CCC: $27.50
Published on Web 04/22/2004

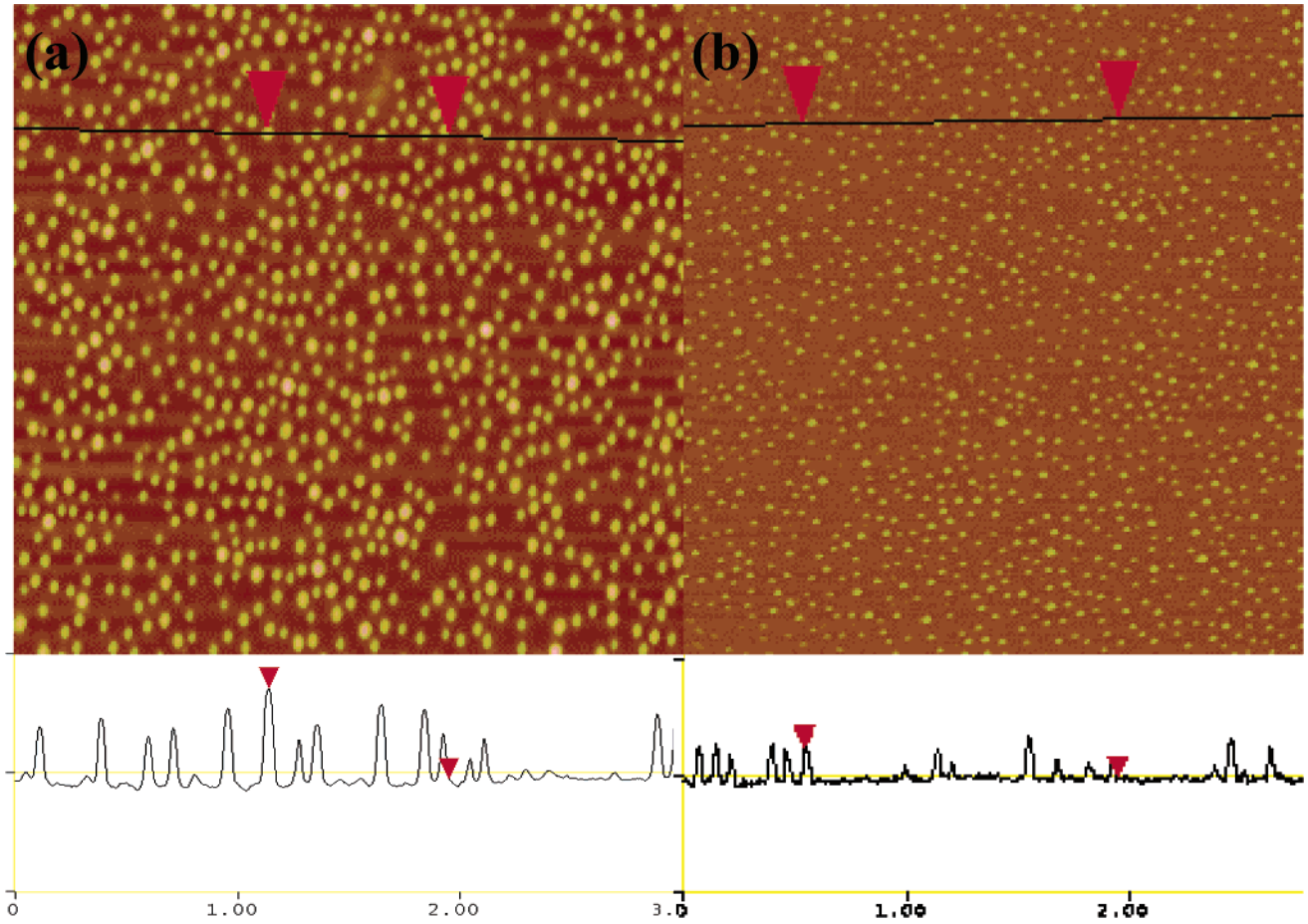

Figure 1. (a) Tapping mode AFM image of the PS−PVP micelles loaded with $FeCl_3$ ($FeCl_3$:PVP = 0.6) dispersed on the surface. The image size is 3 × 3 μm^2. (b) AFM image of the Fe_2O_3 nanoclusters ($FeCl_3$:PVP = 0.6) formed on the surface after the oxygen plasma treatment. The image size is 3 × 3 μm^2.

oxygen plasma (PDC-32G, Harrison) for 15 min. The substrates were further annealed at 700 °C in air for 5 min prior to CVD process.

Chemical Vapor Depositions of SWNTs. The substrates coated with nanoclusters were first put in a 1 in. quartz tube and then heated in 500 sccm H_2 to 900 °C. CH_4 (800 sccm) and C_2H_4 (20 sccm) were then added to the gas flow, and the growth lasted for 10 min. After the growth, CH_4 and C_2H_4 were switched off and the furnace was cooled down to room temperature under the protection of H_2.

AFM Characterizations of the Nanoclusters and SWNTs on the Surface. The substrates with nanoclusters and nanotubes were characterized with a tapping mode atomic force microscope (TPAFM) (Digital Instruments Nanoscope IIIa, Vecco). The diameters of the nanoclusters and nanotubes were determined by measuring the height of nanoculsters and nanotubes on AFM images.

Electrical Characterization of the SWNT Mat on SiO_2/Si Wafer. The electrode was fabricated on top of SWNT mats by using a 50 mesh TEM grid (Ted Pella, Inc.) as a shadow mask. Cr (5 nm) and Au (25 nm) were evaporated as the electrode, and the distance between drain and source electrodes is 40 μm. Highly doped Si underneath the thermal oxides layer was used to apply the back gate.

Results and Discussion

When PS−PVP is dissolved in toluene, the diblock copolymer will self-assemble to form inversed micelles at relatively low concentration. Those micelles consist of cores formed by a polar PVP block and shells formed by the nonpolar PS block. The PS block is preferentially dissolved in toluene and thus shields the PVP cores from the toluene. Thus the PVP core forms a nanocontainer for metal salt within each micelle.[23,24] When solid $FeCl_3$ was added, it could be dissolved in the PVP core of the micelle. Figure 1a shows the TPAFM image of micelles loaded with $FeCl_3$ dispersed on the surface by spin coating. The discrete individual micelles with average diameters of 13.3 nm were evenly dispersed on the surface and formed a monolayer micelle film. It was found that the morphology of the micelle film was closely related to the preparation methods. Simply pulling the wafer from the solutions[23−26] produced a surface with the micelles aggregated to each other (see Supporting Information). However, when spin coating the solutions at high speed (∼8000 rpm), the micelles on the surface formed a uniform monolayer micelle film in a large area. The results suggest that the balance of the speed of solvent evaporations, the adhension between micelles and substrate, and the capillary force applied to the micelle during the evaporation play an important role during the coating process. After the oxygen plasma treatment, all organic components in the micelle were removed and the remaining $FeCl_3$ was converted and formed discrete γ-Fe_2O_3 nanoclusters.[27] Figure 1b shows the AFM image of iron oxide nanoclusters formed on the surface after the plasma treatment. The average diameter of the nanoclusters reduced to 7.9 nm due to the removal of organic shells in micelles. It is obvious that no aggregation happened due to the mild conditions and low temperature in the plasma treatments.

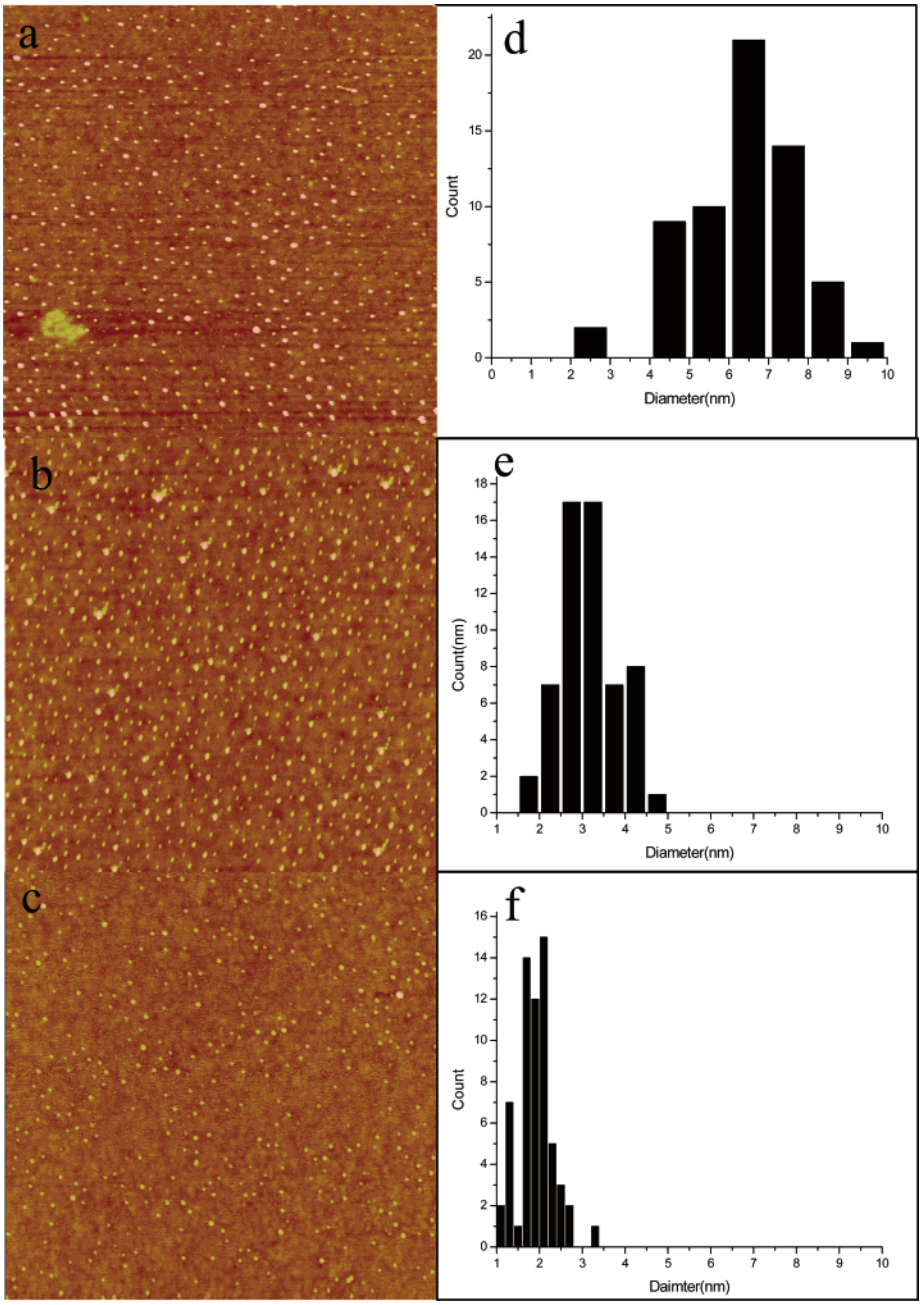

Figure 2. Tapping mode AFM image of nanoclusters formed on the surface with different ratios between $FeCl_3$ and the PVP block: (a) $FeCl_3$:PVP = 0.6; (b) $FeCl_3$:PVP = 0.2; (c) $FeCl_3$:PVP = 0.06. All images are $3 \times 3\ \mu m^2$. Diameter distributions of the nanoclusters formed from (d) $FeCl_3$:PVP = 0.6, (e) $FeCl_3$:PVP = 0.2, and (f) $FeCl_3$:PVP = 0.06.

The size of the nanoparticles could be controlled by the ratio between the $FeCl_3$ and PVP block in the copolymer. Figure 2 shows the AFM images of γ-Fe_2O_3[28] nanoclusters formed on the surface with ratios ($FeCl_3$:PVP) 0.6, 0.2, and 0.06 after oxygen plasma treatment and then annealed at 700 °C in air for 5 min; the average diameters of the nanoclusters are 6.6, 3.0, 1.9 nm, corresponding to the decreasing amount of $FeCl_3$ added. And, meanwhile, the annealing process has caused some shrinkage in the diameters of the nanoclusters from AFM observations. Compared to the oxygen plasma treatment, high temperature is a harsh condition and all the hydrocarbon contaminants on the surface will be completely burned off and thus induce the decrease of the size. However, no aggregation of nanoclusters was observed in the high temperature annealing process. The cluster density also varies with the loading ratio. We believe that this is caused when solution was diluted to obtain the small diameter nanoclusters, it is very difficult to obtain micelles with evenly distributed $FeCl_3$, because it involves the exchange the $FeCl_3$ between different micelles; thus there are still some micelles empty or with low $FeCl_3$ loading. This also shown by the size of nanoclusters not completely reflecting the ratio of the loading.[29] More precise control could be obtained using PS−PVP with a low weight PVP block.[24,25,27] The results clearly demonstrate that by adjusting the ratio between $FeCl_3$ and the PVP block in the copolymer, one can control $FeCl_3$ loaded into the micelle and thus the diameter of the nanoclusters on the surface, and the micelle could be well dispersed on the surface by a suitable procedure such as spin coating.

In the CVD process, it has been shown that diameters of SWNTs could be controlled by the size of the catalyst particles. Here, the nanoclusters transferred to the surface were proven

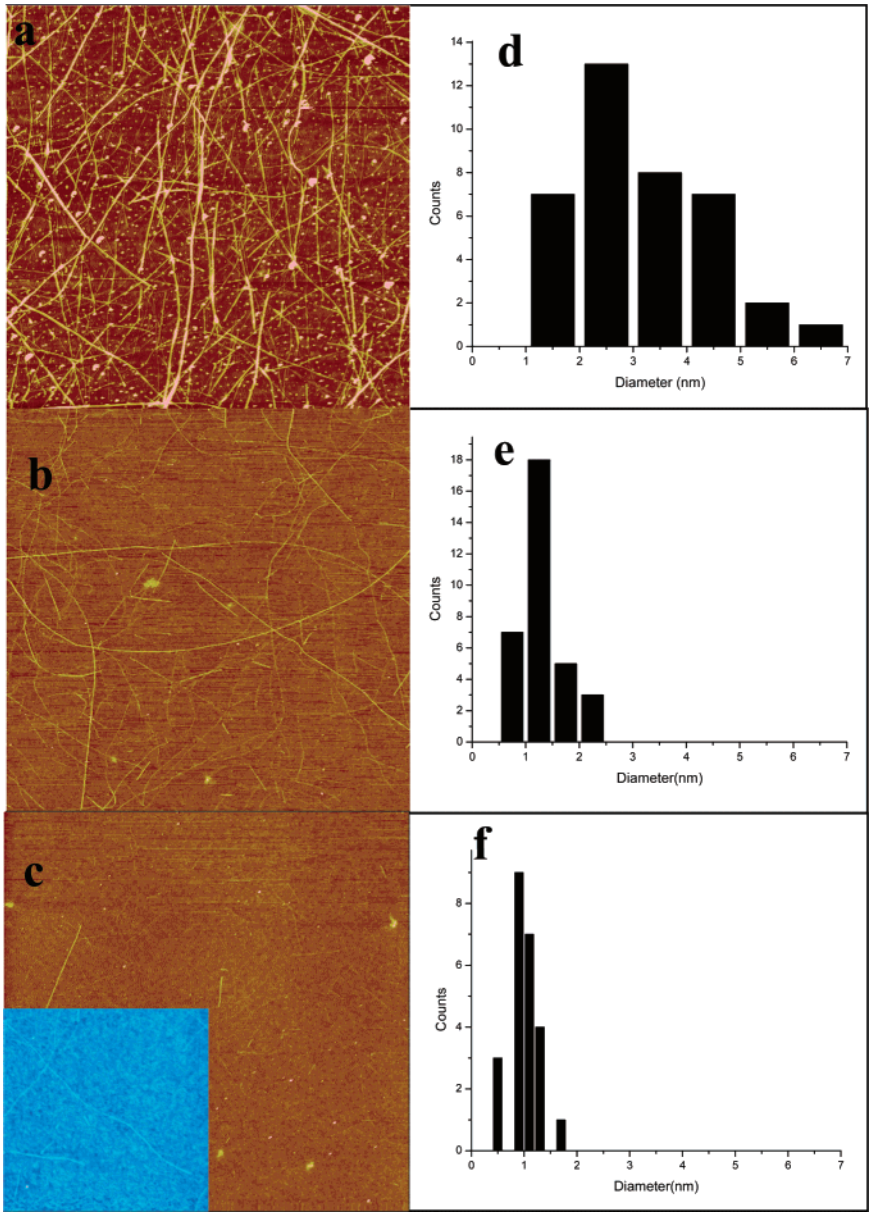

Figure 3. AFM image of nanotubes grown on the surface at 900 °C with different size nanoclusters: (a) $FeCl_3$:PVP = 0.6; (b) $FeCl_3$:PVP = 0.2; (c) $FeCl_3$:PVP = 0.06. All images are $3 \times 3\ \mu m^2$. Diameter distributions of the nanotubes formed from (d) $FeCl_3$:PVP = 0.6, (e) $FeCl_3$:PVP = 0.2, and (f) $FeCl_3$:PVP = 0.06.

to be very good catalysts for growth of SWNTs and also control the diameter. Figure 3 shows the AFM images of SWNTs synthesized from nanoclusters at 900 °C. Due to the high coverage of the nanoclusters on the surface, SWNTs grown on the substrate have a high density, overlapping each other to form continuous mats. All samples with nanoclusters of different diameters have SWNTs on the surface that are long, extend to outside the image area, and overlap with each other to form a complete network of nanotubes on surface (Figure 3a−c). The diameters of the SWNTs on the surface are 2.7 ± 0.3, 1.2 ± 0.1, and 0.9 ± 0.1 nm (Figure 3d−f), and the populations of the SWNTs on the surface decreased when the diameters of the nanoclusters decreased. Compared to the diameter of the nanoculsters, the nanotube diameters are 50% less than the original diameter of the nanoclusters. We believe that there are two possibilities that might contribute to the dimension shrinkage of the nanoclusters and subsequently the diameter of produced nanotubes: First, during the growth process, the γ-Fe_2O_3 nanoclusters were reduced to the Fe^0 state due to the reductive atmospheres when the substrates were heated in H_2, and this could cause the change of the diameter of the nanoclusters during the growth and subsequently the diameter of nanotubes. Second, due to the high growth temperature, metal nanoclusters might evaporate during the growth process and thus the diameters of nanoclusters decrease. Such metal evaporation is also manifested by the morphology change of SWNTs on surfaces when cluster densities decreased. For larger diameter nanoclusters (6.6 nm), we observed a large portion of small diameter SWNTs with broad range distributions (Figure 3d); however, for small diameter nanoclusters the density of SWNTs is much less and the diameter distributions are narrower (Figure 3e,f). Those observations suggest that the catalyst encounters severe evaporation during the growth and big nanoculsters shink to small diameter clusters, thus giving small diameter nanotubes, whereas small nanoclusters evaporate completely because nanoclusters with small diameters evaporate faster. However, due to the random arrangement of nanoculsters on the surface, it is very difficult for us to estimate the degree of the evaporation

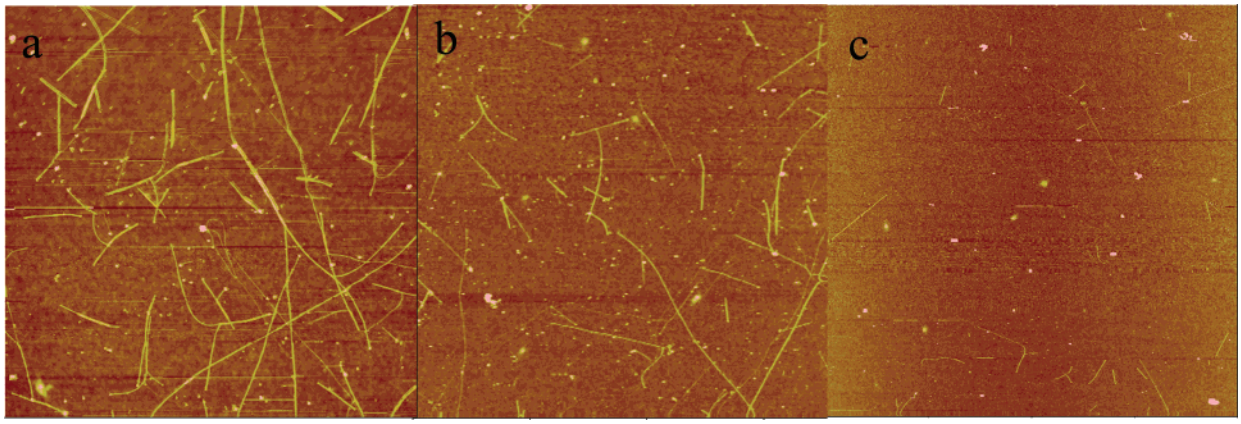

Figure 4. AFM image of the SWNTs grown under different temperature: (a) $FeCl_3$:PVP = 0.2, grown at 800 °C; (b) $FeCl_3$:PVP = 0.06, grown at 800 °C; (c) $FeCl_3$:PVP = 0.06, grown at 700 °C. All images are 3 × 3 μm^2.

and growth efficiency. Further investigations are needed to elucidate those effects in SWNT CVD growth.

Temperature is believed to play a very important role in the SWNT growth. Previously, SWNTs have been synthesized at various temperatures.[20] In our investigations, it was found the growth temperature of the SWNTs is closely related the diameters of the nanoclusters. When the CVD was carried out at 800 °C, for the nanoclusters with average diameter at 6.6 nm, no nanotubes were observed on the surface; however, the nanoclusters with average diameters of 3.0 and 1.9 nm can still act as the catalyst for the growth (Figure 4a,b). Compared with the nanotubes produced at 900 °C, there are a large number of short nanotubes on the surface. The growth temperature can be further decreased to 700 °C but the only catalyst that is still active is nanoclusters with diameters at 1.9 nm. However, the growth efficiency is low and the nanotubes are short (Figure 4c). The dependence on the temperature shows that larger nanoclusters require higher temperature to grow SWNTs. We believe that such growth dependence on temperature suggests that larger nanoclusters require higher temperatures to help the carbon diffusing in the catalyst nanoclusters and the diffusion of the carbon in the catalyst is the control step in the growth. Additionally, larger clusters need to shrink their size to a more appropriate size range to grow nanotubes, which are more accommodated at higher temperatures.

Electrical measurements show that the dense SWNT mats are mixtures of metallic and semiconducting SWNTs. We put a number of electrodes on different positions on the SWNTs mat in an area 3 mm by 3 mm on surface (Figure 5a) and measure the current across the mat while applying gate voltage. Figure 5b shows the change of the current across the mat as function of gate voltage applied through the Si backgate at different positions on the surface. The SWNT mat shows typical p-type semiconductor behavior, and when the gate voltage was scanned from −40 to +40 V, the current across the SWNTs decreased from 2300 to 400 nA. The residue current under the positive gate voltage might be caused by the metallic nanotubes in the mat. At different spots, the electrical properties of the SWNT are similar and the deviations of the on current and off current are less than 20%. The electrical measurement results suggest that the SWNT mats are mixtures of metallic and semiconducting SWNTs and the distributions of the SWNT mats are evenly distributed in large areas on the surface. The observation of such a mixture of semiconducting and metallic SWNTs in CVD agrees with previously reported results.[30] Raman characterizations also confirm the SWNT mats are quite uniform and free of amorphous carbon (see Supporting Information). However, no difference was observed for the SWNTs mats with different diameters in the gate voltage scanning range during the measurements. We believe that this is because there are still quite an amount of small diameter SWNTs even in the SWNT mat from large diameter nanoclusters and those small diameter SWNTs may dominate the turn-off behavior in the

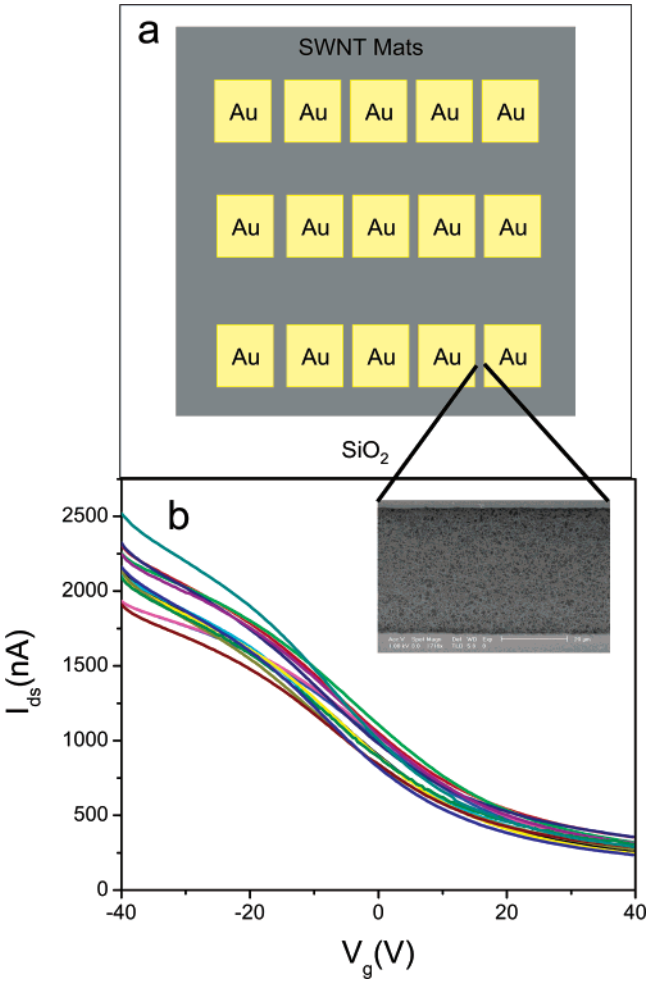

Figure 5. (a) Scheme of the lay-up of electrodes on an SWNT mat (area: 3 × 3 mm^2). The contact length of electrodes with SWNTs is 500 μm, and the gap between electrodes is 40 μm. (b) Source-drain current (I_{ds}) vs back-gate voltage (V_g) for the SWNTs thin film FET fabricated on an SWNT mat (bias: 20 mV). SWNTs mats are synthesized from 6.6 nm nanoclusters at 900 °C. A total of 14 curves were measured on the different neighboring electrodes. Inset: Typical SEM image of the SWNT thin film across the electrodes.

measurements. Nevertheless, the electrical measurements suggest that such high density SWNT mats could be used as building blocks for thin film transistors, chemical sensors, and other potential applications.

Conclusions

In summary, we have successfully loaded iron chloride into inversed micelles formed by PS−PVP in toluene solutions. Those micelles can be easily transferred onto the surface and transformed into Fe_2O_3 nanoclusters after oxygen plasma treatment. The size of the nanoclusters could be easily controlled by the loading ratio between $FeCl_3$ and the PVP block in the copolymer. The different sized nanoclusters could be used as catalysts for SWNT growth. A high density SWNT mat has been directly grown on a flat surface free of amorphous carbon. The diameter of the SWNTs could be controlled by the diameter of the nanoculsters on the surface. Electrical measurements show that mats are mixtures of metallic and semiconducting SWNTs and could be used as building blocks for thin film transistors, chemical sensors, and other potential applications.

Acknowledgment. The project is in part supported by a grant from Army Research Office (DAAD19-00-1-0548), NASA (NAG-1-01061) and 2002 Young Professor Award from DuPont. The authors thank Prof. Eric W. Mcfarland and Dr. Ju Chou at UCSB for the helpful discussion in preparations of the micelle and Prof. Boris B. Akhremitchev for the helpful discussion in experimental details. Prof. Gleb Finkelstein is also thanked for allowing us to use the facilities in his lab.

Supporting Information Available: AFM image of aggregated micelles on substrate. Micro-Raman characteriztions of SWNTs on surface. This material is available free of charge via the Internet at http://pubs.acs.org.

References and Notes

(1) Iijima, S. *Nature* **1991**, *354*, 56.
(2) Saito, R.; Dresselhaus, M. S. *Physcial Properties of Carbon Nanotubes*; Imperial College Press: London, 1998.
(3) Tans, S. J.; Verschueren, A. R. M.; Dekker, C. *Nature* **1998**, *393*, 49.
(4) Kong, J.; Franklin, N. R.; Zhou, C. W.; Chapline, M. G.; Peng, S.; Cho, K. J.; Dai, H. *Science* **2000**, *287*, 622.
(5) Misewich, J. A.; Avouris, Ph.; Tsang, J. C.; Heinze, S.; Tersoff, J. *Science* **2003**, *300*, 783.
(6) Bachtold, A.; Hadley, P.; Nakanishi, T.; Dekker, C. *Science* **2001**, *294*, 1317.
(7) Derycke, V.; Martel, R.; Appenzeller, J.; Avouris, P. *Nano Lett.* **2001**, *1*, 453.
(8) Nygard, J.; Cobden, D. H.; Lindelof, P. E. *Nature* **2000**, *408*, 342.
(9) Bockroath, M.; Cobden, D. H.; Lu, J.; Rinzler, A. G.; Smalley, R. E.; Balents, L.; Mceuen, P. L. *Nature* **1999**, *397*, 598.
(10) Bachtold, A.; Salvetat, J.; Bonard, J.; Forró, L.; Nussbaumber, T.; Schönenberger, C. *Nature* **1999**, *397*, 673.
(11) Novak, J. P.; Snow, E. S.; Houser, E. J.; Park, D.; Stepnowski, J. L.; McGill, R. A. *Appl. Phys. Lett.* **2003**, *83*, 4026.
(12) Chen, R. J.; Bangsaruntip, S.; Drouvalakis, K. A.; Kam, N. W. S.; Shim, M.; Li, Y. M.; Kim, W.; Utz, P. J.; Dai, H. *Proc. Natl. Acad. Sci. USA* **2003**, *100*, 4984.
(13) Snow, E. S.; Novak, J. P.; Campbell, P. M.; Park, D. *Appl. Phys. Lett.* **2003**, *82*, 2145.
(14) Su, M.; Zheng, B.; Liu, J. *Chem. Phys. Lett.* **2000**, *322*, 321.
(15) Huang, S. M.; Cai, X. Y.; Liu, J. *J. Am. Chem. Soc* **2003**, *125*, 5636.
(16) Kong, J.; Soh, H. T.; Cassell, A. M.; Quate, C. F.; Dai, H. *Nature* **1998**, *395*, 878.
(17) Li, Y.; Liu, J.; Wang, Y. Q.; Wang, Z. L. *Chem. Mater.* **2001**, *13*, 1008.
(18) Li, Y. M.; Kim. W.; Zhang, Y. G.; Rolandi, M.; Wang, D. W.; Dai, H. *J. Phys. Chem.* **2001**, *105*, 11424.
(19) Choi, H. C. K.; Wang, D.; Dai, H. *J. Phys. Chem. B* **2002**, *106*, 12361.
(20) Cheung, C. L.; Kurtz, A.; Park, H.; Lieber, C. M. *J. Phys. Chem. B* **2002**, *106*, 2429.
(21) Zheng, B.; Gu, G.; Makarovski, A.; Finkelstein, G.; Liu, J. *Nano Lett.* **2002**, *2*, 895.
(22) Fu, Q.; Lu, C. G.; Liu, J. *Nano Lett.* **2002**, *2*, 329.
(23) Spatz, J. P.; Massmer, S.; Hartmann, C.; Moller, M.; Herzog, T.; Krieger, M.; Boyen, H. G.; Ziemann, P.; Kabius, B. *Langmuir* **2000**, *16*, 407.
(24) Haupt, M.; Miller, S.; Ladenburger, A.; Sauer, R.; Thonke, K.; Spatz, J. P.; Riethmuller, S.; Moller, M.; Banhart, F. *J. Appl. Phys.* **2002**, *91*, 6057.
(25) Jaramillo, T. F.; Baeck, S. H.; Cuenya, B. R.; McFarland, E. W. *J. Am. Chem. Soc.* **2003**, *125*, 7148.
(26) Boyen, H. G.; Kastle, G. Z. K.; Herzog, T.; Weigl, F.; Ziemann, P.; Mayer, O.; Jerome, C.; Moller, M.; Spatz, J. P.; Garnier, M. G.; Oelhafen, P. *Adv. Funct. Mater.* **2003**, *13*, 359.
(27) Sohn, B.; Yoo, S.; Yun, S.; Zin, W.; Jung, J.; Kanehara, M.; Hirata, T.; Teranishi, T. *J. Am. Chem. Soc* **2003**, *125*, 6368.
(28) Carlos Garcia, Y. Z.; Francis, D.; Ulrich, W. *Angew. Chem., Int. Ed.* **2003**, *42*, 1526.
(29) Under the assumption that nanoclusters in sphere shape, the loading ratio of $FeCl_3$ (0.6:0.2:0.06) would give nanoclusters with a diameter ratio of 2.2:1.8:1, and the ratio measured from AFM gives a ratio 2.2:1.5:1.
(30) Kim, W.; Choi, H. C.; Shim, M.; Li, Y.; Wang, D.; Dai, H. *Nano Lett.* **2002**, *2*, 703.